

1 **High-resolution lac insect genome assembly provides genetic insights
2 into lac synthesis and evolution of scale insects**

3 Weiwei Wang^{1,2}, Xiaoming Chen^{1,2*}, Nawaz Haider Bashir¹, Qin Lu¹, Jinwen Zhang¹,
4 Xiaofei Ling¹, Weifeng Ding¹, Hang Chen^{1,2*}

5

6 ¹ Institute of Highland Forest Science, Chinese Academy of Forestry, Kunming 650224, China;

7 ²The Key Laboratory of Cultivating and Utilization of Resources Insects, State Forestry
8 Administration, Kunming 650224, China;

9 *Correspondence: Cafc xm@139.com; stuchen6481@gmail.com

10

11 **Abstract:** Lac insect is an important resource insect with great commercial value.
12 However, the lack of its genome information restricts the fundamental biological
13 research and applied studies of this species. Here, we first assembled the contig of
14 *Kerria lacca* using Illumina and Nanopore sequencing by Hi-C and T2T techniques to
15 obtain the genome of *K. lacca* at the chromosome 0 gap level. The genome of *K.*
16 *lacca* was 256.62 Mb and the Scaffold N50 was 28.53 Mb. A total of 56.94 Mb of
17 repeat sequences, constituting 22.19% of the assembled genome, were identified. We
18 annotated 10,696 protein-encoding genes with 89.74% annotated. By horizontal gene
19 transfer analysis, we obtained a putative gene Isoprenyl diphosphate synthase (IPPS),
20 a key enzyme in the isoprene synthesis pathway in the regulation of lac biosynthesis
21 that transferred horizontally from bacteria to the genome of *K. lacca*. Meanwhile, we
22 constructed the lac synthesis biosynthetic pathway and screened 25 putative key genes
23 in the synthesis pathway by transcriptome analysis in different developmental stages
24 and tissues. It provides new research ideas to reveal the molecular mechanism of lac
25 biosynthesis and regulation. The high-quality chromosomal-level genome of lac insect
26 will provide a basis for the study of development, genetics, and the evolution of scale
27 insects.

28 **Keywords:** *Kerria lacca*, Isoprenyl diphosphate synthase, Lac synthesis, Horizontal
29 gene transfer

30 **1. Introduction**

31 *Kerria* spp. is a herbivorous insect of the order Hemiptera (Coccoidea,
32 Tachardiidae), with 29 species worldwide (Varshney and Sharma, 2020; Talukder and
33 Das 2020; Rajgopal et al., 2021; Bashir et al., 2021), and the majority of them found
34 in tropical and subtropical regions of south Asia and southeast Asia between
35 70-120 °E and 8-32 °N (Varshney and Sharma, 2020). *K. lacca* has become an
36 important insect species for producing high-quality lac because of its high lac resin
37 content, low wax, less impurities, and light color, and it is an important forest
38 resource insect in a country. Lac insects can parasitize over 300 host plant species,
39 such as *Schleichera oleosa*, *Flemingia macrophylla* and *Cajanus cajan*, and suck host
40 plant phloem using piercing-sucking mouthparts. Simultaneously, females secrete the
41 secondary metabolite lac through glands (Chen and Feng, 2009).

42 Shellac is the only animal-secreted natural resin that has been extensively
43 researched and utilized in a wide range of ways; its primary components are shellac
44 resin, shellac wax, and shellac dye. Lac resin is a mixture of lactones and lactides
45 derived from hydroxy-fatty acids and sesquiterpene esters; among them, the
46 hydroxy-fatty acid is mainly aleutric acid, whereas the sesquiterpene acid is primarily
47 jalaric acid (Chen et al., 2008, Chen et al., 2021). Because of its exceptional qualities
48 such as strong adhesion, good insulation, strong plasticity, moisture resistance,
49 corrosion resistance, and smooth coating, shellac is considered an important natural
50 forest chemical raw resource. It is frequently utilized after processing in the military
51 industry, chemical industry, electronics, food, medicine, and other industries with
52 significant economic significance (Chen, 2005; Thombare et al., 2022). Moreover,
53 due to the fact that it is natural, non-toxic, biodegradable, and good for the
54 environment, it can also be used as an eco-friendly material and has a lot of potential
55 for green technology. Researchers predicted that the shellac industry will require
56 about 7,500-8,000 tons of shellac and its value-added products annually, resulting in
57 economic benefits of 80-90 million US dollars (Thombare et al., 2022).

58 Extensive research on lac insects has been conducted both domestically and

59 internationally, with a focus on their biological characteristics, ecological adaptability,
60 host plants, genetic variety, and so on; however, research on the mechanism of lac
61 synthesis is still lacking. In their investigation of genes associated with lac resin
62 production, Shamim et al. discovered that acetyl-CoA is a common precursor for the
63 synthesis of jalaric acid and sesquiterpene acid. A transcriptomic study of *K. chinensis*
64 at different developmental stages screened 28 candidate genes related to lac synthesis,
65 verified the function of the screened FAD gene, and found that this gene has a
66 regulatory effect on lac secretion (Wang et al., 2019a, 2019b). At present, the rule of
67 lac secretion by lac insect and the molecular mechanism of lac formation in the body
68 are unclear, and effective methods to improve the quantity and quality of lac secreted
69 by lac insect have not been discovered, which has become a barrier in the
70 development of the lac industry both at home and abroad. Understanding the
71 molecular regulation mechanism of lac biosynthesis is of great significance for
72 optimizing lac insect secretion and establishing sustainable and effective lac
73 production.

74 Here, we report the first high-quality genome assembly of the lac insect. In this
75 study, we used high-quality whole genome data of the lac insect *K. lacca*, along with
76 transcriptome analysis of different development stages and tissues, to
77 comprehensively explore the mechanism of lac synthesis. The findings of this study
78 have the potential to increase the genetic information of scale insects, further
79 elucidate the molecular regulation mechanism of lac biosynthesis, and also be used as
80 a valuable resource in the development, genetics, and evolution of Kerriidae. This
81 lays a molecular foundation for the protection, improvement, and exploitation of lac
82 insect genetic resources.

83 2. Materials and methods

84 2.1 Samples

85 Samples of *Kerria lacca* were reared on *Schleichera oleosa* at the Experimental
86 Station of Yuanjiang, Institute of Highland Forest Science, Chinese Academy of

87 Forestry in Yunnan Province, China (102°00'46" E, 23°36'11" N). Female lac insects
88 at late adult (n = 100) stages were collected. To perform transcriptome analysis of
89 different developmental stages and adult tissues, female lac insects larvae (n =100),
90 early adults (n = 100), mid adults (n =100), and late adults (n = 100) were collected.
91 Additionally, four tissue samples were obtained from females at the late adult stage
92 (A3) using a sterilized scalpel and tweezers: anal tubercle (AT), brachia (BH), body
93 wall (BW) and midgut (MG). Reactions were carried out in three replicates for each
94 biological sample. Immediately, all samples were put in liquid nitrogen, then
95 transferred and stored at -80 °C. The samples were used for DNA and RNA extraction,
96 library construction, and sequencing.

97 **2.2 Genomic sequencing**

98 Genomic DNA (gDNA) was isolated from 100 individual female lac insects at
99 late adult stages using the CTAB method, following the manufacturer's instructions.
100 After measuring quality and quantity, a library with an average insert size ~150 bp
101 was constructed and sequenced using the Illumina NovaSeq 6000 (Illumina, San
102 Diego, CA, USA) platform. For third-generation sequencing, a library with an
103 average insert size ~15 Kb was constructed. The libraries were sequenced on the ONT
104 (Oxford Nanopore Technologies, Oxford, UK) Sequel platform with Sequel
105 PromethION P48. For Hi-C analysis, 100 lac insect specimens were soaked in 1%
106 formaldehyde for 10 min at room temperature and in a 2.5 M-glycine solution to
107 terminate the isolation and cross-linking of lac insect cells. After adaptor ligation and
108 quality control, the Hi-C library was sequenced using the Illumina HiSeq PE150
109 platform.

110 **2.3 Genomic assembly**

111 The Illumina paired-end reads were used for 19 bases k-mer analysis to estimate
112 the genome size and heterozygosity. To construct the chromosome-level genome
113 assembly, the Hi-C sequencing data were aligned to the final assembled contigs by
114 ALLHiC (v0.9.12) and juicer (v1.6) (Neva et al., 2016b) to obtain the interaction

115 matrix, and then the contigs were sorted and anchored using 3D-DNA (v180419)
116 (Dudchenko et al., 2017). Finally, the Hi-C contact maps were applied to the 3D-DNA
117 visualization module and reviewed with juicebox Assembly Tools (v1.11.08) (Neva et
118 al., 2016a) for quality control and interactive correction of the automatic output. A
119 chromosome-level genome sequence was obtained by using 100 N complement gaps
120 from sequenced, directed, and non-redundant contig sequences. For genome assembly,
121 the clean Nanopore reads after filtering and decontamination were assembled with
122 Next Denovo (<https://github.com/Nextomics/NextDenovo/releases/tag/v2.3.1>). To fix
123 sequencing errors in the final assembly, Racon (version: 1.4.11) and Pilon (version:
124 1.23) were chosen to polish the genome using long sequencing data and short reads
125 with default parameters for two rounds each. In order to obtain a 0 gap genome, we
126 respectively combined the ONT raw data and wtdbg assembly method to obtain a
127 contig level genome using winnowmap (v1.11, parameter: k=15, -- MD) (Chirag et al.,
128 2020) approach connects to the nextdenovo skeleton containing Gap, crosses the Gap
129 and replaces sequences containing Gap regions to obtain a T2T level genome.

130 The location and number of genome gaps were used to determine the continuity
131 of genomic assembly. The second-generation sequencing clean reads were compared
132 to the reference genome using bwa (version: 0.7.17-r1188). The consistency of the
133 assembled genome was evaluated by comparing the ratio and coverage of the
134 second-generation sequencing. Then, BUSCO (version: 4.1.4; eval=1e-05) was
135 used to assess the genome's completeness and accuracy.

136 **2.4 Gene annotation**

137 Repeat elements were identified using RepeatModeler (version: open-1.0.11,
138 BuildDatabase -name mydb;RepeatModeler -database mydb -pa 10) (Smit et al. 2015)
139 and LTR_FINDE (version: official release of LTR_FINDER_parallel, -threads 16,
140 -harvest_out, -size 1000000, -time 300) to construct a denovo repeat sequence
141 database. Based on denovo repetitive sequence libraries and the RepBase library
142 (<http://www.girinst.org/repbase>) (Smit et al., 2015), using RepeatMasker (version: the
143 open - 4.0.9, -nolow-no_is-norna-parallel 2) (Smith et al., 2013) repeated annotation;

144 RepeatProteinMask (version: open-4.0.9, -nolowsimplex -pvalue 0.0001) predicts the
145 repeat sequence of TE_protein type. All the repeats identified by different methods
146 were combined into the final combined TEs after removing the redundant repeats.

147 Genome structure analysis was conducted using homology-based prediction,
148 transcriptome-based prediction, and de novo prediction. For homology annotation,
149 protein sequences of five closely related species, including *Aphis_gossypii*,
150 *Acyrthosiphon_pisum*, *Bemisia_tabaci*, *Diaphorina_citri*, and *Diuraphis_noxia*, were
151 downloaded from the National Center for Biotechnology Information database (NCBI)
152 and used for annotation through genewise Exonerate (version: v2.4.0) ([Slater and](#)
153 [Birney, 2005](#)). For the denovo prediction, Augustus (version: 3.3.2) and Genscan
154 (version: 1.0) ([Salzberg et al., 1998](#)) were employed to annotate gene structures. For
155 transcript annotation, the transcriptome data were aligned to the assembled genome
156 using TransDecoder (version: v5.1.0), and nonredundant transcripts were obtained
157 using Stringtie (version: 2.1.1). All the gene models were processed by MAKER
158 (version: 2.31.10) ([Holt and Yandell, 2011](#)) to obtain the final gene set.

159 Gene function was annotated by searching the protein databases Uniprot
160 ([Apweiler et al., 2004](#)), the Kyoto Encyclopedia of Genes and Genomes (KEGG)
161 (<http://www.genome.jp/kegg/>) ([Kanehisa and Goto, 2000](#)), InterProScan (version:
162 5.52-86.0) ([Blum et al., 2021](#)), NR ([Deng et al., 2006](#)), KOG, and GO with blastp
163 (version: 2.0.11.149, E- value <1e-5) ([Buchfink et al., 2015](#)). tRNAscan-SE (version:
164 1.23) ([Chan et al., 2021](#)) was used to annotate the noncoding RNA for tRNA
165 screening and RNAmmer (version: 1.2) was used for sequence alignment with
166 homologous species to identify rRNA. The Rfam database was used with the
167 INFERNAL (version: 1.1.2) ([Nawrocki and Eddy 2013](#)) software to predict ncRNAs
168 in the genome.

169 2.5 Phylogenetic analysis

170 A total of 16 insects were selected to construct a phylogenetic tree: *K. lacca*,
171 *Ericerus pela*, *Phenacoccus solenopsis*, *B. tabaci*, *Nilaparvata lugens*, *Cimex*

172 *lectularius*, *D. noxia*, *A. pisum*, *Drosophila melanogaster*, *Anopheles gambiae*,
173 *Bombyx mori*, *Danaus plexippus*, *Tribolium castaneum*, *Anoplophora glabripennis*,
174 *Nasonia vitripennis*, and *Daphnia pulex*. Protein sequences for these species were
175 constructed with the **orthofinder** (version: 2.3.12, -M msa) pipeline using the default
176 parameters.

177 We generated multiple sequence alignments for each 1:1 orthologous cluster
178 using Muscle (Edgar, 2004). We used trimal (version: v1.4.rev22, -gt 0.2) to remove
179 positions with gaps in more than 20% of the aligned sequences and concatenated all
180 1:1 orthologous genes in each species into a super-sequence. The phylogenetic tree
181 was constructed using the maximum-likelihood method implemented in RAxML
182 (version: 8.2.10) (Model: PROTGAMMAWAG) for branch support. Support values
183 were obtained from 1,000 bootstrap replicates. Meanwhile, divergence time and age
184 of fossil records were derived from TimeTree (<http://www.timetree.org/>) and applied
185 as the calibration points. According to the divergence times from TimeTree, the nodal
186 dates of *D. pulex* and *B. tabaci* were 452-557 million years ago (MYA), those of *E.*
187 *pela* and *A. glabripennis* were 334-394 MYA, *N. lugens* and *A. pisum* were 177-401
188 MYA, *A. gambiae* and *D. plexippus* were 243-317 MYA, and those of *K. lacca* and *D.*
189 *noxia* were 150.9-271.1 MYA.

190 Gene family expansion or contraction analysis was performed using CAFE
191 (version: 4.2) (Han et al., 2013) based on the results of the **orthofinder** and the
192 phylogenetic tree. The accepted level for indicating significantly altered gene families
193 was $p < 0.05$.

194 **2.6 Positive selection analysis**

195 We generated protein sequence alignments for single-copy gene families using
196 MAFFT (localpair-maxiterate 1000). Then PAL2NAL (version: v14) was used to
197 invert the protein sequence into a codon alignment sequence. The CodeML program
198 from the PAML (version: 4.9i) package was implemented to estimate the dN/dS
199 (nonsynonymous to synonymous) ratio for genes with the branch-specific model and

200 the branch-site model. The likelihood ratio tests (LRTs) were used to compare the
201 tested Model A (which allows positive selection on each of the foreground lineages,
202 $\omega > 1$) with the null model, which does not allow such positive selection. The results of
203 a significant difference ($p < 0.05$) were designated as “positively selected genes.”

204 **2.7 HGT event identification**

205 For *K. lacca*-specific HGTs, we submitted 10,696 predicted coding genes of *K.*
206 *lacca* to a BLASTP search against the NCBI protein database (E-value= 1×10^{-5}). The
207 proteins with the best BLAST hits in bacterial or fungal sequences were extracted,
208 and the number of extracted sequences was counted to obtain the position and
209 sequence information of HGT genes on the genome. After sequences without support
210 from transcript evidence were excluded, a series of parameters were used to filter the
211 candidates, including the sequences that were further compared to the NR library; the
212 alignment consistency was 30-70%, the sequence length was >150 bp, and the q
213 coverage was $>50\%$. All candidate HGTs were subjected to phylogenetic analysis for
214 verification. Synonymous codon-usage order values and GC contents of HGT and
215 non-HGT genes were calculated by CodonO.

216 **2.8 RNA sequencing and transcriptome assembly**

217 Total RNA was extracted separately from L, A1, A2, A3, BH, BW, AT, and MG
218 samples using the R6814 Blood RNA Kit (Life Technologies) following the procedure
219 provided. RNA quantity, purity, and integrity were determined on a NanoPhotometer
220 and an Agilent 2100 Bioanalyzer. Libraries were constructed using an Illumina
221 NEBNext® UltraTM RNA Library Prep Kit according to the manufacturer's
222 instructions and sequenced on an Illumina Novaseq 6000 platform. Clean reads were
223 mapped to the genome assembly using Star (version: 2.7.9a, default) ([Dobin et al., 2013](#)).
224 Differentially expressed genes were identified by $\text{padj} < 0.005$ and log2 (fold
225 $\text{change)} > 1$. GO and KEGG enrichment was performed using clusterProfiler (version:
226 3.14.3) ([Yu et al., 2012](#)).

227 **2.9 Predicting the putative lac biosynthesis pathway**

228 Lac biosynthesis requires hydroxy-fatty acids and sesquiterpene esters, all of
229 which participate in fatty acid biosynthesis and terpenoid biosynthesis. We used the
230 KEGG PATHWAY and ORTHOLOGY tools in the Kyoto Encyclopedia of Genes and
231 Genomes (KEGG) to detect all participating components and the KEGG orthology.
232 Based on differential expression gene analysis in different developmental stages and
233 different tissues, orthomcl version 2.0.9 with default parameters was used to detect
234 orthologous groups of lac biosynthesis KOs in the sequenced *K. lacca* genome. blastp
235 (E- value <1e- 5) was used to determine the locations of the Kos. All steps related to
236 lac biosynthesis were linked, and a KEGG pathway was proposed for lac biosynthesis.

237 *K. lacca* samples were prepared from different developmental stages (L, A1, A2,
238 and A3) and different tissues (BH, BW, AT, and MG). Total RNA was extracted from
239 the mixed sample of *K. lacca* using the EZ-10 Total RNA Mini-Preps Kit (Sangon
240 Biotech, Shanghai, China) according to the manufacturer's instructions. The
241 first-strand cDNA was synthesized using the NovoScript Plus All-in-One 1st Strand
242 cDNA Synthesis SuperMix (gDNA Purge) (Novoprotein Scientific Inc., Shanghai,
243 China) according to the manufacturer's protocol. Specific primers for the genes on the
244 biosynthesis pathway of lac were designed using Primer Premier 6.0 (**Table S16**). In
245 this study, the qPCR was performed using the NovoStart SYBR qPCR SuperMix Plus
246 Kit (Novoprotein Scientific Inc.). The reactions were run on an ABI Quant Studio 3
247 real-time PCR system (Applied Biosystems, Thermo Fisher Scientific, Waltham, MA,
248 USA). The gene expression levels were calculated with the $2^{-\Delta\Delta CT}$ method ([Livak and](#)
249 [Schmittgen 2001](#)).

250 **3 Results**

251 **3.1 Genome assembly**

252 We adopted Illumina and Oxford Nanopore Technologies sequencing for the
253 comprehensive analysis of the *K. lacca* genome. A total of 68.06 GB of clean data
254 was generated using the Illumina platform. The k-mer (K=19) analysis indicated that
255 the heterozygosity of *K. lacca* was 0.27% and the estimated genome size was 262.92

256 Mb (**Table 1**, **Figure S1**, **Table S2**). The sequencing of the Oxford Nanopore
257 Technologies, Oxford, UK platform generated 124.67 Gb raw data. After removing
258 low-quality and short reads, we obtained 116.66 Gb of clean reads for genome
259 assembly: a data set of 9,127,577 reads with an N50 of 34,324 bp (**Table S1**). A draft
260 genome assembly of 258.04 Mb was obtained, yielding 26 contigs with a contig N50
261 of 23,848,510 bp.

262 Then, we used Hi-C long-range scaffolding to improve our assembly. A total of
263 108.35 Gb of raw data was generated, and 92.73 Gb of filtered clean reads were used
264 for the following analysis (**Table S1**). As a result, the chromosome-level genome has
265 a total length of 256.62 Mb, with a scaffold of N50 of 28.53 Mb (**Table 1**). One
266 hundred percent of the genome's bases were successfully anchored to the nine
267 chromosomes (**Figure S2**, **Table S3**). Chromosome lengths ranged from 24,084,477
268 bp to 33,948,441 bp. Through T2T assembly technology, we finally obtained a
269 high-quality genome with 0 gaps.

270 To assess assembly accuracy, we remapped the Illumina paired-end reads to the
271 assembled genome. The reads mapped to 99.72% of the assembled genome sequences
272 with a 99.23% mapping rate and 261.19 \times average sequence depth (**Table S6**).
273 Furthermore, 1,307 (95.7%) of the 1,367 highly conserved insect orthologues from
274 BUSCO were identified in the assembly (**Table S5**). As revealed by BUSCO analyses
275 against the Insecta datasets, the *K. lacca* genome assembly contained a higher number
276 of conserved single-copies than the four published insect genomes (**Figure S3**).
277 Together, these results suggest the completeness and high quality of our genome
278 assembly.

279 We evaluated the genome of *K. lacca*. The survey result indicates that the proportion
280 of commensal bacteria contamination was extremely high, and the effective data was
281 only 22%. In order to remove the contamination of the lac insects, we adopted the
282 strategy of increasing the sequencing volume, and the genome sequencing depth of
283 the lac insects was 450 X, so as to ensure that the effective depth of assembly was 100
284 X. Nextdenovo's assembly and comparison with NT showed that most of the

285 sequences were aligned to the *K. lacca* genome. The GC_depth plot has no abnormal
286 peak shape and conforms to the Poisson distribution, so the contamination cannot be
287 investigated by the GC_depth plot alone (Figure S4). Then we used interaction signals
288 in Hi-C to find the location of commensal contamination. The Hi-C-assisted assembly
289 results show that the overall quality of our genome is high, but the last small piece of
290 scaffold has a strong interaction signal of its own but no interaction with the rest of
291 the genome, so we predicted that the last scaffold is contaminated with bacterial genes.
292 To verify that it was a commensal contamination, NT alignment was performed on the
293 last scaffold (named ctg000120_P) sequence with a length of 1,433,897 bp, and the
294 results were mapped to the symbiotic bacteria *Wolbachia pipiensis*. To further confirm
295 the ctg000120_P contamination sequence for commensal bacteria that should be
296 removed, we assembled the *Wolbachia pipiensis* genome of size 1,539,149 bp. The
297 1,539,149 bp commensal sequences were compared with the 1,433,897 bp
298 ctg000120_P with MiniMAP2, and 1,093,096 bp sequences of the 1,433,897 bp were
299 found to be able to map the reassembled commensal sequences. Meanwhile, we used
300 the assembled bacterial genome and the contig-level genome to compare with
301 minimap2. Interestingly, there were 521,296 bp sequences that could be mapped to the
302 reassembled symbiotic sequences, and their genome locations in lac insects were all
303 chimeric within contigs with an extremely low proportion, which suggests that
304 ctg000120_P may be caused by horizontal gene transfer (HGT) rather than bacterial
305 contamination. In conclusion, the bacterial sequence found in the genome is the result
306 of HGT and pollution, with a 32.29% chance that it was generated by HGT and a
307 67.71% chance that it was caused by pollution.

308 3.2 Genome annotation

309 A total of 79,136,004 bp of repetitive sequences were obtained in the *K. lacca*
310 genome, yielding a repeat percentage of 22.19% (Table S7). *K. lacca* had far fewer
311 repetitive sequences than the closely related species *Ericerus pela* (37.3%) and
312 *Phenacoccus solenopsis* (37.9%) (Chen et al., 2021; Li et al., 2020). We integrated
313 expression data from eight RNA-seq libraries, homolog protein alignment, and de

314 novo gene prediction to create 10,696 protein-coding genes in *K. lacca*. The average
315 CDS length, exon number per gene, exon length, and intron length were 1,342.95 bp,
316 6.97 bp, 269.31 bp, and 1,321.07 bp, respectively, similar to those in most of the
317 reported scale insect species (**Table S8**). This BUSCO analysis indicated that the
318 annotated gene-sets have a completeness value of 94.2% (**Table S5**). Among the
319 10,696 predicted genes, 9,599 (89.74%) were functionally annotated, including 9,199
320 (86.00%) genes found via the Interproscan database, 8,850 (82.74%), and 8,839
321 (82.64%) genes via the NR and Uniprot databases, respectively (**Table S9**).

322 **3.3 Gene orthologues and comparative genomic analysis**

323 We used the OrthoMCL to identify orthologous genes among *K. lacca* and 15
324 other insect species. A total of 37,306 gene family clusters were constructed, with 446
325 identified as 1:1:1 single-copy orthologous genes (**Table S12**). In addition, we also
326 identified 880 *K. lacca* specific gene families. Using the protein-coding sequences of
327 446 single-copy orthologous genes (*Daphnia pulex* as an outgroup), a phylogenetic
328 tree was constructed. The results showed that *K. lacca* and seven other Hemiptera
329 were clustered together. Scale insects (including *K. lacca*, *E. pela*, and *D. pulex*) and
330 Aphididae (including *Diuraphis noxia* and *Acyrthosiphon pisum*) diverged from their
331 common ancestor about 169.4 million years ago (MYA) (156.5~178.5 MYA). *K.*
332 *lacca* was a sister taxon to *E. pela*. The two scale insect species diverged from their
333 common ancestor at approximately 57.9 MYA (44.6~70.3 MYA). Further, our
334 analysis indicated that the last common ancestor of holometabola and incomplete
335 metamorphosis separated in the Late Devonian 389.5 (372.6~409.3 MYA), at least 80
336 million years earlier than the previous study ([Misof et al., 2014](#); [Chen et al., 2021](#)).
337 Based on this phylogenetic analysis, ametabolous insects represent a primitive group
338 located in the basal branch of the tree, whereas Hemiptera and holometabola reside
339 separately in the lower and upper branches. Three scale insects (*K. lacca*, *E. pela*, and
340 *D. pulex*) are an important transitional taxon between incomplete metamorphosis and
341 holometabola. This similarity to a previous report supports an evolutionary trend from
342 ametabolous to incomplete metamorphosis insects, followed by the emergence of

343 holometabola (Chen et al., 2021) (Figure 2-B).

344 Significant expansion and contraction of gene families are usually related to the
345 adaptive divergence of species. Three scale insects showed 375 expanded and 65
346 contracted gene families compared with those of the common ancestor of (*K. lacca*, *E.*
347 *pela*, and *D. pulex*) and two Aphididae (*Diuraphis noxia* and *Acyrtosiphon pisum*),
348 while the *K. lacca* genome displayed 258 expanded and 622 contracted gene families
349 compared with those of the common ancestor (Figure 2-B). We analyzed the
350 functional properties of the expanded 258 gene family (758 genes), and KEGG and
351 GO enrichment analysis revealed that the identified 70 gene expansion might be
352 related to enriching the nutrient metabolism pathway of the lac insect. The expanded
353 gene families were involved in Lysosome (11), vitamin digestion and absorption (10),
354 fat digestion and absorption (10), glycerolipid metabolism, and so on. Because of its
355 piercing sucking mouthpiece, the lac insect can only absorb a limited amount of
356 nutrients from its host plants. The expansion of nutrition metabolism genes might
357 facilitate the digestion and absorption of nutrients from plant hosts. In addition, 80
358 genes were significantly enriched in categories primarily involved in xenobiotic
359 detoxification, such as carboxylic ester hydrolase activity (22), oxidoreductase
360 activity (19), monooxygenase activity (19), ABC transporters (10), and so on. The
361 expansion of genes might facilitate the detoxification of natural xenobiotics from
362 plants (Figure 2-C, Figure S6-B).

363 Three groups of 47 genes involved in the *K. lacca*-specific related gene also
364 underwent expansion. Among them, four genes expanded that were functionally
365 related to terpenoid biosynthesis. This might be because lac insect species produce a
366 large amount of lac, which is an effective adaptation for *K. lacca* to escape predators
367 and cope with harsh environmental conditions. In addition, 24 genes involved in heme
368 binding and 24 genes involved in an iron ion binding-related gene also underwent
369 expansion; this might be related to the red pigment synthesis of the lac insect (Figure
370 2-C, Figure S6-A).

371 **3.4 Positive selection analysis**

372 To further uncover the genomic characteristics of *K. lacca*, a positive selection
373 analysis was performed. Using 446 single-copy gene families, 49 positive selection
374 genes (PSGs) (FDR < 0.05) were identified. GO and KEGG enrichment analysis, we
375 found that 11 PSGs participated in pathways that may be associated with nutrition
376 metabolism, such as the amino acid metabolism (aspartate aminotransferase (AST)),
377 glycerophospholipid metabolism (phospholipase), and glycan biosynthesis (glucoside
378 xylosyltransferase). Moreover, PSGs were also related to the cell cycle, RNA
379 transport, and ribosome formation. Amino acids in insect haemolymph play a key role
380 in providing energy through osmosis, proline metabolism, neurotransmission, and
381 other metabolic pathways (Klowden, 2007; Mirhaghparast et al., 2015). There are
382 reports that AST is a sign of the entrance of amino acids into the glucogenesis process
383 (Lehninger, 1982). Gluconeogenesis is the main pathway for sugar synthesis from
384 non-carbohydrate substrates (Etebari et al., 2007). In this series of reactions, the
385 carbon source of gluconeogenesis is amino acids, and the activation of this metabolic
386 pathway is usually related to the large reduction of free amino acids in fat bodies and
387 hemolymph. At this time, alanine is converted into pyruvate to provide energy
388 (Matindoost et al., 2005; Hasheminia et al., 2011). We analyzed the aspartate
389 aminotransferase (AST) gene, which is a positive selection in the genome. It was
390 composed of 428 amino acids. On the basis of 59 AST protein sequences from three
391 scale insects and other insects, we constructed a phylogenetic tree. The gene
392 phylogeny strongly supported the interspecific relationships demonstrated in a
393 previous tree based on species classification analyses (Figure 2-A). In the analysis of
394 the AST amino acid sequence of *K. lacca*, it was found that it contained multiple
395 conserved domains, including the unique conserved domain of the aspartate
396 aminotransferase supergene family. We then identified shared amino acid
397 substitutions that occurred along the lineage containing scale insects *K. lacca*, *E. pela*,
398 and *D. pulex*, but not along the lineages leading to the Hemiptera (*Acyrthosiphon*
399 *pisum*, *Aphis gossypii*, *Diuraphis noxia*, *Rhopalosiphum maidis*, *Schlechtendalia*
400 *chinensis*), Thysanoptera (*Thrips palmi*), and Diptera (*Polypedilum vanderplanki*)
401 species. We speculate that amino acid substitution in the conserved domain of the

402 three scale insects might contribute to energy conversion and thus provide energy
403 (Figure 2-B).

404 **3.5 Horizontal gene transfer**

405 Horizontal gene transfer is a significant dynamic of genome evolution in both
406 prokaryotic and eukaryotic organisms, and it is accompanied by adaptive evolution
407 (Li et al., 2022). We used a variety of methods to identify the genes that may cause
408 HGT in *K. lacca*. First, 27 candidate genes were compared to fungi or bacteria
409 through protein-coding genes of the genome and compared to the NR library by blast.
410 Then, 16 candidate genes were obtained through screening genes supported by
411 transcripts. Finally, the above sequences were compared to the NR library, where the
412 alignment consistency was 30-70%, the sequence length was >150 bp, and the q
413 coverage was greater than 50%, yielding 5 genes that underwent HGT events.

414 Candidate gene *Kerria0046210.1* encodes Isoprenyl diphosphate synthases (IPPS)
415 through achieving comparison in the NR library. The phylogenetic tree of Isoprenyl
416 diphosphate synthases (IPPS) of 23 species was constructed by blast and RAXML.
417 The result that the gene from *K. lacca* and *Corynebacterium tapiri* formed a branch
418 and had a close affinity shows the gene may undergo horizontal gene transfer (Figure
419 2-C). The GC content calculated by CodonO of the gene is higher than that of
420 adjacent upstream and downstream genes (Table S13). Transcriptome analysis in
421 different developmental stages and tissues showed the gene has high expression in
422 each stage and tissue of *K. lacca*. The PCR results showed that the *Kerria 0046210.1*
423 gene existed in *K. lacca* (Figure 2-D). The protein encoded by the gene is composed
424 of 242 amino acids. The analysis of the amino acid sequence of *Kerria 0046210.1*
425 showed that it had a conserved domain of the cis-isopentenyl transferase family using
426 the NCBI's Sequence Conservative Domains (CD) search tool. Previous studies have
427 shown that IPPS is a key enzyme connecting the biosynthetic branching points of
428 upstream mevalonate and downstream isoprene (Wang and Ohnuma, 2000; Chen et
429 al., 2021). The back of the body wall (BW), anal tubercle (AT), and the brachia (BH)
430 process with more glands have higher expression compared with the midgut without

431 glands in different tissues through differential gene analysis ([Figure 2-E](#)). Therefore,
432 isopentenyltransferase plays an important role in the process of terpenoid skeleton
433 biosynthesis and regulation, and it may be the key gene for lac synthesis.

434 **3.6 The putative lac biosynthesis pathway**

435 To construct a putative lac biosynthetic pathway in *K. lacca*, two related KEGG
436 pathways were analyzed: fatty acid synthesis and terpenoid biosynthesis. Comparative
437 genomic analysis of *K. lacca* showed that 3 of the genes that were related to fatty acid
438 biosynthesis and 4 genes involved in terpenoid biosynthesis underwent expansion in
439 the expansion gene family. Furthermore, we used transcriptome analysis to screen 25
440 key candidate genes in the lac biosynthesis pathway in different developmental stages
441 and tissues. The different developmental stages that the lac secretion-active adult
442 stages have in comparison with the lac secretion-minimum larval stage, in the process
443 of lac biosynthesis, 11 genes were differentially expressed. Different tissues with
444 more glands, BH, BW, and AT, had 14 genes with differential expression when
445 compared to glandless MG. There were 10 candidate genes related to terpenoid
446 biosynthesis and 15 related to fatty acid biosynthesis. The q-PCR results of the above
447 key genes were basically consistent with the expression profile found with RNA-seq
448 ([Figures 3-A and 3-B](#)). Based on these analyses, we proposed a putative pathway for
449 lac biosynthesis. Though further validation is required, this putative pathway
450 integrates most steps of lac biosynthesis, which is a useful resource for elucidating the
451 biosynthesis mechanism of lac ([Figure 3-C](#)).

452 **4 Discussion**

453 Scale insects contain a large number of endosymbiotic bacteria ([Baumann, 2005](#);
454 [Szabó et al., 2017](#); [Kandasamy et al., 2022](#)), which poses a great challenge to getting
455 high-quality genomes. In this study, we increased the amount of sequencing and then
456 assembled the genome at the contig level for GC_ depth map, NT library pair, and
457 interaction signal in Hi-C to obtain a high-quality genome from lac insect
458 contaminated by a large number of symbiotic bacteria as well as a portion of
459 horizontally transferred genes. In order to get rid of symbionts contamination and get

460 horizontally transmitted genes, this will provide a new strategy for subsequent
461 sequencing of scale insects and their highly contaminating species.

462 Horizontal gene transfer (HGT) is the transfer of genetic information from one
463 organism to another via indirect inheritance in prokaryotes, phagocytic cells, and
464 parasitic unicellular eukaryotes (Gladyshev et al., 2008). Insects inherit most of their
465 horizontally transferred genes from bacteria and fungi, followed by a few viruses and
466 plants. HGT is accompanied by the adaptive evolution of insects and plays an
467 important ecological role in the functional adaptation of insects. For example, the
468 carotenoid biosynthesis gene was transferred from fungi to aphids, which can change
469 the body color of aphids (Moran and Jarvik, 2010); the whitefly detoxifying ability
470 was enhanced by phenolic glycoside genes obtained from plants (Xia et al., 2021); the
471 parasitoid killing factor (PKF) gene was introduced to Lepidoptera from a virus to
472 increase their defenses (Gasmi et al., 2021); and the LOC105383139 gene, which was
473 transferred from a bacterium to *Plutella xylostella* to enhance male-female courting
474 behavior (Li et al., 2022). Scale insects include a large number of endosymbionts that
475 are important in their nutrition and metabolism (McCutcheon and Moran, 2012;
476 Husnik et al., 2013). These symbionts play key roles in the biology of their host
477 insects, providing nutrients like essential amino acids and vitamins that the insects are
478 unable to produce (Baumann, 2005; Douglas, 1989; Moran, 2007). During the
479 long-term evolution of symbiotic bacteria and insects, several genes from symbiotic
480 bacteria were horizontally transferred to the insect genome and carried out their
481 biological functions. We found an IPPS gene that had been horizontally transferred
482 from bacteria into the scale insect. Studies have shown that isopentenyl transferase
483 (IPPS), also known as *Hevea* rubber transferase (HRT), is found in the final step of
484 natural rubber biosynthesis and is a key enzyme in rubber biosynthesis. Its family can
485 interact with farnesyl pyrophosphate (FPP), SRPP, HRBP, and REF to regulate the
486 activity of these essential proteins, and so it plays an important role in the regulation
487 of rubber biosynthesis (Lou et al., 2009; Yamashita et al., 2016; Tang et al., 2016). In
488 the rubber biosynthesis of *Hevea brasiliensis*, rubber particles (RPs) are special

489 organelles for rubber biosynthesis and storage, and the most abundant proteins on the
490 RPs membrane are IPP, Z-IPPS, small rubber particle protein (SRPP), and rubber
491 elongation factor (REF), of which Z-IPPS is a significant large component that
492 impacts not only the speed of rubber biosynthesis but also the production of latex
493 (Wang et al., 2010; Liu et al., 2020). Researchers found that IPPS is involved in
494 rubber synthesis in the rubber-producing plant (*Taraxacum koksaghyz*), and its
495 activity is positively correlated with rubber production (Schmidt et al., 2010). Eight
496 IPPS genes were identified in its genome, and one of them, IPPS1, is highly expressed
497 in latex, providing more target genes for subsequent specific functional studies of
498 IPPS genes (Li et al., 2017; Xie et al., 2019). Unlike the rubber tree, which produces
499 *cis*-polyisoprene, *Eucommia ulmoides* rubber biosynthesis depends on the
500 *trans*-isopentenyl transferase E-IPPS, in which the farnesyl diphosphate synthases
501 (FPS) plays a role in the synthesis of natural *trans* rubber as E-IPPS (Wuyun et al.,
502 2017). Therefore, the IPPS gene, which was horizontally transferred from bacteria
503 into the scale insect genome, is a key enzyme that connects the biosynthetic sites of
504 upstream mevalonate and downstream isoprene, plays an important role in the
505 biosynthesis and regulation of terpenoid backbones, and might be a key gene of lac
506 synthesis. In-depth investigation of the specific biological function of IPPS in the
507 regulation of lac biosynthesis in lac insects will lead to new insights for elucidating
508 the precise mechanism of lac biosynthesis and secretion.

509 Based on Illumina and ONT sequencing platforms, Hi-C technology, and T2T
510 assembly, we provide the genome of *K. lacca* at chromosome level 0 Gap. The
511 phylogeny suggests that *K. lacca* diverged from a common ancestor with *E. pelta*
512 57.94 MYA. Among the expanded 258 gene families, 197 genes related to nutrition
513 metabolism, detoxification and *K. lacca*-specific were identified, and positive
514 selection occurred in AST genes related to nutrient metabolism in positive selection
515 analysis. By transcriptome analysis of different developmental stages and tissues, 25
516 candidate genes related with *K. lacca* synthesis were screened, among which IPPS
517 genes from bacteria were integrated into the *K. lacca* genome via horizontal gene

518 transfer, and the biosynthetic pathway of *K. lacca* was constructed. This study will
519 provide a basis for the analysis of the unique nutritional metabolism mechanism, as
520 well as genetic and evolutionary studies of the scale insect.

521 **Acknowledgements**

522 The research was supported by the grant for Fundamental Research Funds of CAF
523 (CAFYBB2020QA003), National Natural Science Foundation of China (31772542)
524 and grants for the high level foreign experts introduced to Yunnan province
525 (YNQR-GDWG-2019-011).

526 **Author contributions**

527 X.M.C. and H.C. designed and led the project. W.W.W. and N.H.B. collected samples.
528 W.W.W., Q.L. and W.F.D. accomplished the whole-genome sequencing and Hi-C
529 assembly. W.W.W., H.C., Q.L., and W.F.D. performed whole-genome assembly
530 quality control and transcriptome analyses. W.W.W., J.W.Z. and X.F.L afforded photos
531 of fresh collection and designed the figures; W.W.W., N.H.B., Q.L. and H.C. wrote
532 the manuscript. X.M.C. and H.C. cowrote and edited the manuscript. All authors read
533 and approved the final manuscript.

534 **Data availability statement**

535 The datasets generated and analysed during the current study are available in the
536 Sequence Read Archive repository (SRA; <https://www.ncbi.nlm.nih.gov/sra/>). The
537 RNA-seq data generated in this study have been submitted to the NCBI BioProject
538 database (<https://www.ncbi.nlm.nih.gov/sra/PRJNA896359>) under accession number
539 PRJNA896359. Hi-C data (the chromosome-level assembly) have been submitted to
540 the Sequence Read Archive (SRA; <http://www.ncbi.nlm.nih.gov/bioproject/922917>)
541 under accession number PRJNA922917. The final DNA sequence assembly has been

542 deposited at DDBJ/ENA/GenBank under the accession LAC00000000.

543 **References**

544 Apweiler R, Bairoch A, Wu CH et al. UniProt: The universal protein knowledgebase. Nucleic
545 acids research, 2004, 32, D115-D119.

546 Ashburner M, Ball CA, Blake JA, et al. Gene ontology: Tool for the unification of biology. Nature
547 genetics, 2000, 25, 25-29.

548 Bashir NH, Wang WW, Liu J et al. First record of the lac-producing species *Kerria nepalensis*
549 Varshney (Hemiptera, Kerriidae) from China, with a key to Chinese species. ZooKeys,
550 2021,1061: 1-9.

551 Baumann P. Biology bacteriocyte-associated endosymbionts of plant sap-sucking insects. Annual
552 Review of Microbiology, 2005, 59, 155-189. <https://doi.org/10.1146/annurev.micro.59.030804.121041>

554 Blum M, Chang HY, Chuguransky S et al. The InterPro protein families and domains database: 20
555 years on. Nucleic acids research, 2021, 49, D344-D354.

556 Buchfink B, Xie C, and Huson DH. Fast and sensitive protein alignment using DIAMOND.
557 Nature methods, 2015, 12, 59-60.

558 Chan PP, Lin BY, Mak AJ et al. tRNAscan-SE 2.0: Improved detection and functional
559 classification of transfer RNA genes. BioRxiv, 2021, 614032.

560 Chen H, Lu Q, Chen XM et al. Genome assembly and methylome analysis of the white wax scale
561 insect provides insight into sexual differentiation of metamorphosis in hexapods. Molecular
562 Ecology Resources, 2021, 21 (6): 1983-1995. <https://doi.org/10.1111/1755-0998.13376>

563 Chen H, Wang WW, Bashir N.H. The heredity and evolution of lac insects. Science Press, Beijing,
564 China, 2021.

565 Chen XM, Feng Y. Chapter 1. Lac insects. In An introduction to resource entomology; Science
566 Press, Beijing, China, 2009, pp. 12-28.

567 Chen XM. Biodiversity of Lac Insects, Yunnan Science and Technology Press, Yunnan, China,
568 2005.

569 Chen Y, Zhu PH, Li R et al. Research Progress of Plant Prenyltransferases. *Biotechnology bulletin*,
570 2021, 37(2):13.

571 Chen, XM, Chen YQ, Zhang H et al. Lac insects breeding and Lac processing. *Chinese Forestry*
572 Press, Beijing, China. 2008.

573 Chirag J, Arang R, Zhang H, et al. Weighted minimizer sampling improves long read mapping.
574 *Bioinformatics*, 2020, (Supplement_1): Supplement_1. 10.1093/bioinformatics/btaa435

575 DengY, Li J, Wu S, et al. Integrated nr database in protein annotation system and its localization.
576 *Comput Eng*, 2006, 32, 71-72.

577 Dobin A, Davis CA, Schlesinger F, et al. STAR: ultrafast universal RNA-seq aligner.
578 *Bioinformatics*, Oxford University Press, 2013, 29, 15-21.

579 Douglas AE. Mycetocyte symbiosis in insects. *Blackwell Publishing Ltd*, 1989, 64(4):409-434.

580 Dudchenko O, Batra SS, Omer AD, et al. De novo assembly of the *Aedes aegypti* genome using
581 Hi-C yields chromosome-length scaffolds. *Science*, 356 (6333): 92-95.

582 Edgar, RC. MUSCLE: Multiple sequence alignment with high accuracy and high throughput.
583 *Nucleic Acids Research*, 2004, 32(5), 1792-1797. <https://doi.org/10.1093/nar/gkh340>

584 Etebari K, Matindoost L, Mirhoseini S Z et al. The effect of BmNPV infection on protein
585 metabolism in silkworm (*Bombyx mori*) larva. *Invertebrate Survival Journal*, 2007,
586 4(1):13-17.

587 Gasmi L, Sieminska E, Okuno S et al. Horizontally transmitted parasitoid killing factor shapes
588 insect defense to parasitoids. *Science*, 2021, 373, 535-541.

589 Gladyshev EA, Meselson M, Arkhipova IR. Massive horizontal gene transfer in bdelloid rotifers.
590 *Science*, 200, 8320, 1210-1213.

591 Han M V, Thomas G W C, Jose L M et al. Estimating Gene Gain and Loss Rates in the Presence
592 of Error in Genome Assembly and Annotation Using CAFE3. *Molecular Biology &*
593 *Evolution*, 2013, (8):1987-1997.

594 Hasheminia SM, Sendi JJ, Jahromi KT et al. The effects of *Artemisia annua* L. and *Achillea*
595 *millefolium* L. crude leaf extracts on the toxicity, development, feeding efficiency and
596 chemical activities of small cabbage *Pieris rapae* L. (Lepidoptera: Pieridae). *Pesticide*
597 *Biochemistry & Physiology*, 2011, 99(3):244-249.

598 Holt C, Yandell M. MAKER2: An annotation pipeline and genome-database management tool for

599 second-generation genome projects. *BMC bioinformatics*, 2011, 12, 1-14.

600 Husnik F, Nikoh N, Koga R et al. Horizontal gene transfer from diverse bacteria to an insect
601 genome enables a tripartite nested mealybug symbiosis. *Cell* 2013, 153, 1567-1578.

602 Kandasamy T, Ekba S, Kumari K et al. Unraveling bacterial diversity of the Indian Lac Insect
603 *Kerria lacca* (Kerr) using next generation sequencing. *International Journal of Tropical Insect
604 Science*, 2022 <https://doi.org/10.1007/s42690-022-00758-x>

605 Kanehisa, M., and Goto, S. KEGG: Kyoto encyclopedia of genes and genomes. *Nucleic acids
606 research*, 2000, 28, 27-30.

607 Klowden MJ. *Physiological Systems in Insects*, Academic Press, 2007, p. 697.

608 Li B, Hu P, Zhu LB et al. DNA methylation is correlated with gene expression during diapause
609 termination of early embryonic development in the silkworm (*Bombyx mori*). *Interactional
610 Journal of Molecular Science*, 2020, 21(2), 671.

611 Li T, Xu X, Ruan J et al. Genome analysis of *Taraxacum kok-saghyz* Rodin provides new insights
612 into rubber biosynthesis. *Natl. Sci. Rev.* 2017, 5, 78-87.

613 Li Y, Liu ZG, Liu C et al. HGT is widespread in insects and contributes to male courtship in
614 lepidopterans. *Cell*, 2022, 185 (16): 2975-2987. <https://doi.org/10.1016/j.cell.2022.06.014>.

615 Liu J, Shi C, Shi CC et al. The Chromosome-Based Rubber Tree Genome Provides New Insights
616 into Spurge Genome Evolution and Rubber Biosynthesis. *Molecular Plant*, 2020, 13(2),
617 336-350.

618 Livak KJ, Schmittgen TD. Analysis of relative gene expression data using real-time quantitative
619 PCR and the $2^{-\Delta\Delta CT}$ Method. *Methods*, 2001, 4: 402-408.

620 Matindoost KSZML, Matindoost L. A study on interaspecific biodiversity of eight groups of
621 silkworm (*Bombyx mori*) by biochemical markers. *Insect Science*, 2005, 12(2):87-94.

622 McCutcheon JP, Moran NA. Extreme genome reduction in symbiotic bacteria. *Nature Reviews
623 Microbiology*, 2012, 10, 13-26.

624 Mirhaghparast SK, Zibaee A, Sendi JJ et al . Immune and metabolic responses of *Chilo
625 suppressalis* Walker (Lepidoptera: Crambidae) larvae to an insect growth regulator,
626 hexaflumuron. *Pesticide Biochemistry and Physiology*, 2015, 125, 69-77.
627 <https://doi.org/10.1016/j.pestbp.2015.05.007>.

628 Misof B, Liu S, Meusemann K, et al. Phylogenomics resolves the timing and pattern of insect
629 evolution. *Science*, 2014, 346(6210), 763-767.

630 Moran NA, and Jarvik T. Lateral transfer of genes from fungi underlies carotenoid production in
631 aphids. *Science*, 2010, 328, 624-627.

632 Moran NA. Symbiosis as an adaptive process and source of phenotypic complexity. *Proceedings*
633 *of the National Academy of Sciences of the United States of America*, 2007, 104(Suppl 1),
634 8627-8633.

635 Nawrocki EP, Eddy SR. Infernal 1.1: 100-fold faster RNA homology searches,” *Bioinformatics*.
636 2013, 29, 2933-2935.

637 Neva CD, James TR, Muhammad S. Juicebox Provides a Visualization System for Hi-C Contact
638 Maps with Unlimited Zoom. *Cell Systems*, 2016, 3 (1): 99-101.
639 <https://doi.org/10.1016/j.cels.2015.07.012>.

640 Rajgopal NN, Mohanasundaram A, Sharma KK. A new species of lac insect in the genus *Kerria*
641 Targioni Tozzetti (Hemiptera: Coccomorpha: Tachardiidae) on *Samanea saman* (Fabaceae)
642 from India. *Zootaxa*, 2021, 4938(1): 60-68.

643 Salzberg S, Searls D, Kasif S. Modeling dependencies in pre-mRNA splicing signals.
644 *Computational methods in molecular biology*, 1998, 129.

645 Schmidt T, Hillebrand A, Wurbs D et al . Molecular cloning and characterization of rubber
646 biosynthetic genes from *Taraxacum kok-saghyz*. *Plant Molecular Biology Reporter*, 2010,
647 28(2): 277-284.

648 Shamim G, Pandey DM, Ramani R et al. Identification of genes related to resin biosynthesis in the
649 Indian lac insect, *Kerria lacca* (Hemiptera: Tachardiidae). *International Journal of Tropical*
650 *Insect Science*, 2014, 34(2): 149-155.

651 Slater GSC, Birney E. Automated generation of heuristics for biological sequence comparison.
652 *BMC bioinformatics*, 2015, 6, 1-11.

653 Smit A, Hubley, Green P. “RepeatModeler open-1.0 (2008-2015),” Seattle, USA: Institute for
654 Systems Biology. 2015. Available from: <http://www.repeatmasker.org>.

655 Smith A, Hubley R, Green P. “RepeatMasker open-4.0,” RepeatMasker Open-4.0. 2013

656 Szabó G, Schulz F, Toenshoff E et al. Convergent patterns in the evolution of mealybug symbioses
657 involving different intrabacterial symbionts. ISME J 2017, 11, 715-726.
658 <https://doi.org/10.1038/ismej.2016.148>

659 Talukder B, Das BK. A new invasive species of *Kerria* Targioni-Tozzetti (Hemiptera:
660 Coccomorpha: Kerriidae) on rain tree, *Albizia saman* (Fabaceae) from India. Oriental insects,
661 2020, 1-15.

662 Tang CR, Yang M, Fang YJ et al. The rubber tree genome reveals new insights into rubber
663 production and species adaptation. Nature Plants 2016, 2, 16073.
664 <https://doi.org/10.1038/nplants.2016.73>

665 Thombare N, Kumar S, Kumari U et al. Shellac as a multifunctional biopolymer: A review on
666 properties, applications and future potential. International Journal of Biological
667 Macromolecules, 2022, 15, 203-223. <https://doi.org/10.1016/j.ijbiomac.2022.06.090>

668 Varshney RK, Sharma KK. Lac insects of the world-an updated catalogue and bibliography. 2020,
669 ICAR-IINRG, Speedo Print, Ranchi, India.

670 Wang KC, Ohnuma SI. Isoprenyl diphosphate synthase. Molecular and Cell Biology of Lipids,
671 2000, 1529, 33-48.

672 Wang WW, Liu PF, Ling XF et al. Construction of RNA interference vector and function analysis
673 of FAD gene in *Kerria chinensis*. Forest Research, 2019b, 32(6):7.

674 Wang WW, Liu PF, Lu Q et al. Potential Pathways and Genes Involved in Lac Synthesis and
675 Secretion in *Kerria chinensis* (Hemiptera: Kerriidae) Based on Transcriptomic Analyses.
676 Insects, 2019a, 10(12).

677 Wang X, Shi M, Lu X et al. A method for protein extraction from different subcellular fractions of
678 laticifer latex in *Hevea brasiliensis* compatible with 2-DE and MS. Proteome Science, 2010,
679 8(1):35-35.

680 Wuyun TN, Wang L, Liu H et al. The Hardy Rubber Tree Genome Provides Insights into the
681 Evolution of Polyisoprene Biosynthesis. Molecular Plant. 2018, 11, 429-442.
682 <https://doi.org/10.1016/j.molp.2017.11.014>

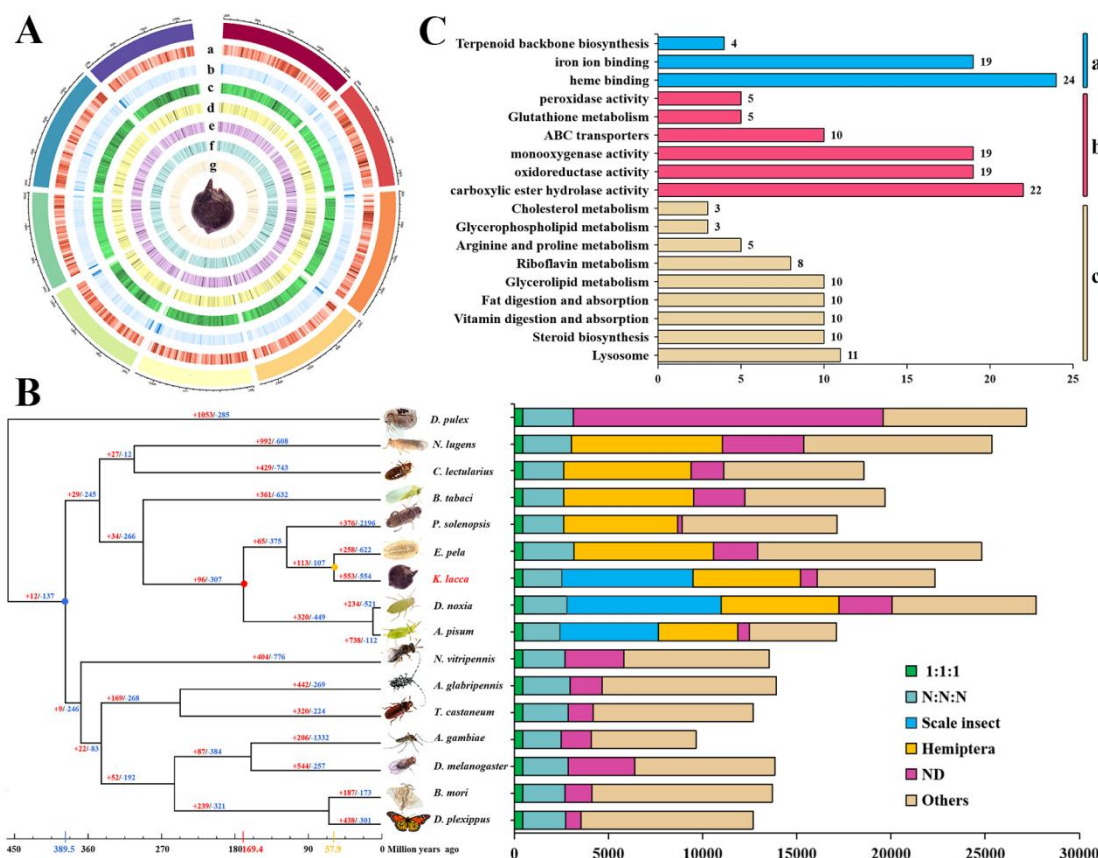
683 Xia J, Guo Z, Yang Z, et al. Whitefly hijacks a plant detoxification gene that neutralizes plant
684 toxins. Cell 2021, 184, 1693-1705.e17.

685 Xie QL, Ding GH, Zhu LP et al. Proteomic landscape of the mature roots in a rubber-producing
686 grass *Taraxacum koksaghyz*. International Journal of Molecular Sciences, 2019, 20, 2596.
687 <https://doi.org/10.3390/ijms20102596>.

688 Yamashita S, Yamaguchi H, Waki T et al. Identification and reconstitution of the rubber
689 biosynthetic machinery on rubber particles from *Hevea brasiliensis*. eLife, 2016, 5: e19022.

690 Yu G, Wang LG, Han Y, et al. clusterProfiler: an R package for comparing biological themes
691 among gene clusters. Omics-a Journal of Integrative Biology, 2012, 16(5):284-287.

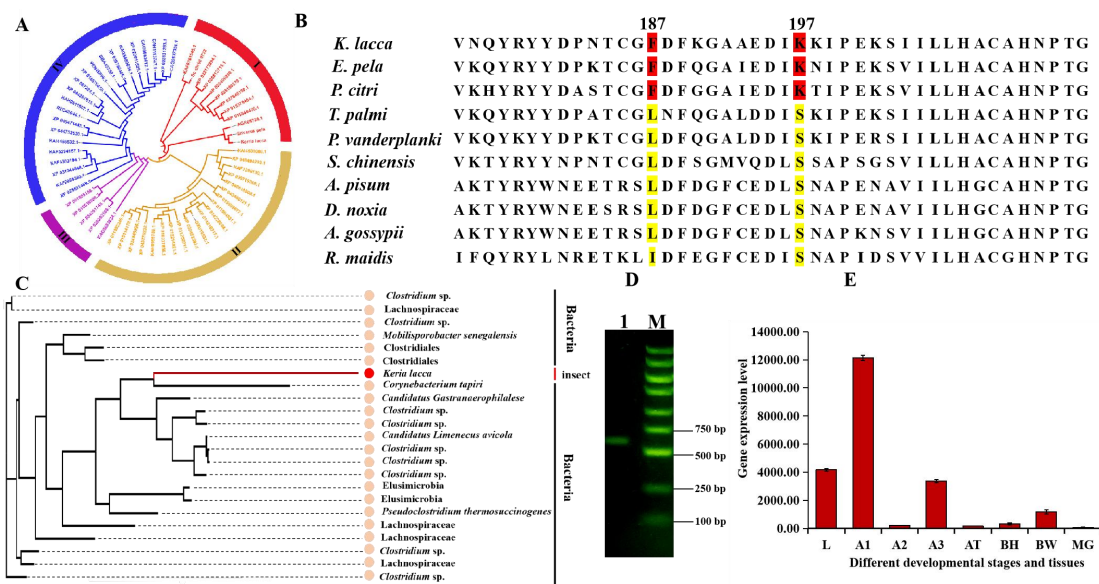
692



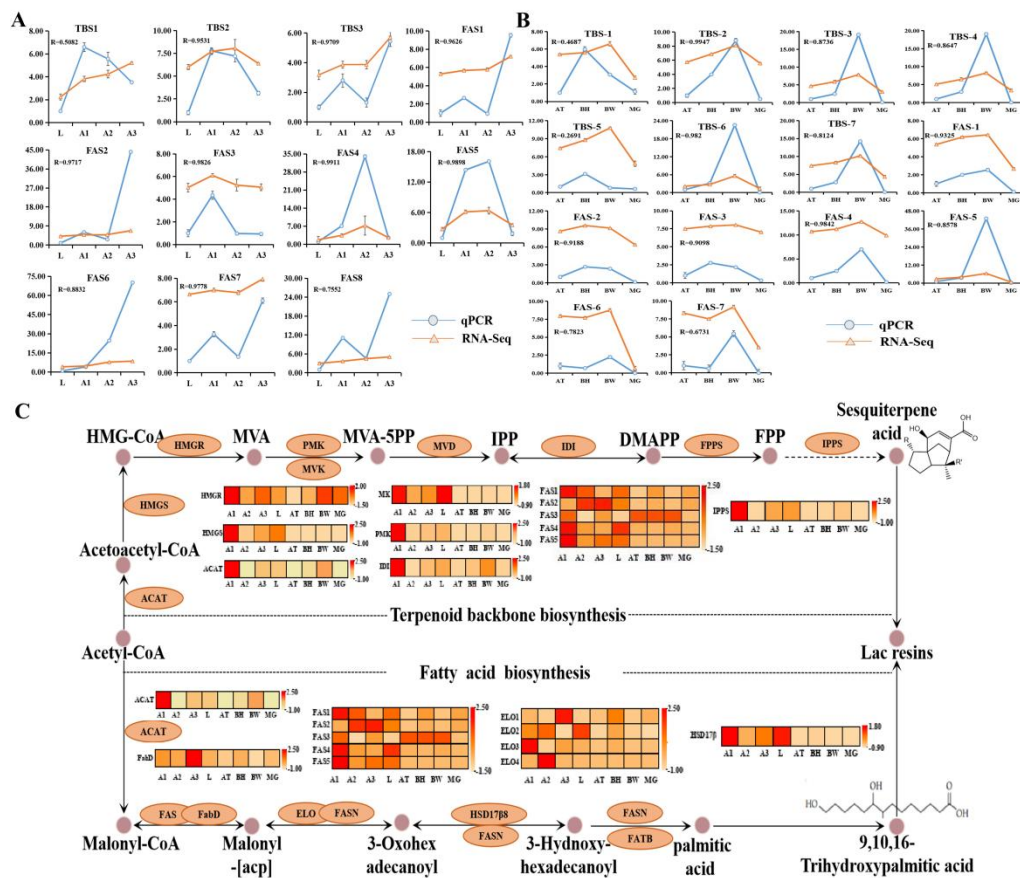
693

694 **Figure 1 Genome evolution of *Kerria lacca*.** **A.** Distribution of *K. lacca* genomic features.
695 Track a-c: gene density (50 kb window), repeats density (50 kb window), and GC content (50 kb
696 window). Track d-g: Mean expression of annotated genes calculated as lg^{FPKM} of the mean
697 expression value in different developmental stages (A1, A2, A3, and L). **B.** Phylogenetic analysis
698 of *K. lacca* with other insect species. The phylogenetic position of *K. lacca* was determined based
699 on 446 single-copy genes. The estimated species divergence time is illustrated at the bottom of the
700 phylogenetic tree. The gene family expansion (red) and contraction (blue) are illustrated at the
701 branches and nodes of the tree. The blue dot and number indicate the divergence time of the
702 incomplete metamorphosis separated from the holometabolous, red color show the time of scale
703 insect diverge from aphids and those in orange color indicate the time of *K. lacca* diverge from *E.*
704 *pela*. 1:1:1 indicates single copy genes, and N:N:N indicates multicopy genes across 16 insect

705 species. The Scale insects and Hemiptera indicate suborder-specific genes, respectively. C.
706 Enrichment analysis of expanded genes of *K. lacca*. a. *K. lacca*-specific related genes. b.
707 Detoxification genes. c. Nutritional metabolism-related genes.



708
709 **Figure 2 Positive selection and Horizontal gene transfer.** A. Phylogenetic tree of the AST gene
710 in *K. lacca* and 58 other insects. B. Alignment of three scale insects and seven other insects AST
711 amino acid sequences. Amino acids unique to the three scale insect species (corresponding to
712 residues 187 and 197 in other insects AST) are shown in red; other amino acids at these positions
713 are shown in yellow. C. Maximum likelihood phylogenetic analysis of IPPS. D. Genome
714 fragments cloned from *K. lacca* IPPS. M, DNA marker; 1, PCR products of the IPPS gene
715 fragment. E. Gene expression levels of IPPS in different development stages and tissues.



716

717 **Figure 3 Comparative transcriptomic analysis of genes involved in the lac biosynthetic**
718 **pathway.** A. Genes expressed differentially at different developmental stages. B. Genes expressed
719 differentially at different tissues. The horizontal represents different developmental stages and
720 tissues of the lac insect. The numbers on the vertical axis represent gene expression for the
721 respective genes. C. Comparative transcriptomic analysis of genes involved in the lac biosynthetic
722 pathway of *K. lacca* from different developmental stages and different tissues.

723

724 **Table 1 Statistics of the *K. lacca* genome assembly**

| Features | Statistics |
|-----------------------|------------|
| Genome size (Mb) | 256,62 |
| Assembly level | Chromosome |
| Number of chromosomes | 9 |
| GC content (%) | 25.40% |
| Contig N50 (Mb) | 23,848,510 |
| Scaffold N50 (Mb) | 28,529,763 |
| BUSCO Insecta (%) | 95.7% |
| Protein-coding genes | 10,696 |

725